GEOPHYSICAL RESEARCH LETTERS, VOL. 33, L12103, doi:10.1029/2005GL025612, 2006

Kinetic aspects of foreshock cavities

Steven J. Schwartz,[1] David Sibeck,[2] Mark Wilber,[3] Karim Meziane,[4] and Timothy S. Horbury[1]

Received 24 December 2005; revised 14 April 2006; accepted 22 May 2006; published 23 June 2006.

[1] We have investigated the kinetic signatures within, and at the edges of, a foreshock cavity. Such cavities are believed to be formed when an isolated collection of interplanetary magnetic field lines connect to quasi-parallel regions of the Earth's bow shock, allowing energetic ions to flow upstream and excavate a local cavity. Observations by the Cluster spacecraft show precisely this configuration. The suprathermal ions can be seen just outside the edges of the cavity within a restricted range of gyrophases, consistent with their gyromotion tangential to the layer containing the cavity. Foreshock cavities, if sufficiently common, may play significant roles in triggering magnetospheric events. Thus our confirmation of their relatively simple formation mechanism lends support to their inferred frequency. **Citation:** Schwartz, S. J., D. Sibeck, M. Wilber, K. Meziane, and T. S. Horbury (2006), Kinetic aspects of foreshock cavities, *Geophys. Res. Lett.*, *33*, L12103, doi:10.1029/2005GL025612.

1. Introduction

[2] Kinetic effects within the foreshock can significantly modify the solar wind shortly before its interaction with the Earth's bow shock. Two categories of events have been observed: hot flow anomalies (HFAs) and foreshock cavities. The former occur at the intersection of certain tangential discontinuities with the Earth's bow shock. Inward pointing electric fields trap reflected ions in the vicinity of the discontinuities. The result is to substantially heat and deflect the thermal ion population within the HFAs. The enhanced thermal pressure can drive shocks at the edges which divert and compress the oncoming solar wind flow [*Schwartz et al.*, 1985; *Thomsen et al.*, 1986]. The flow within the HFA is highly deflected from the Sun-Earth line.

[3] Foreshock cavities are less prominent, but perhaps far more common, than HFAs [*Sibeck et al.*, 2002, 2004]. Unlike HFAs, they are not associated with interplanetary discontinuities separating regions with significantly different field orientations and plasma parameters, although they do possess some local internal structure which is probably related to their pre-event interplanetary conditions. The thermal solar wind ion distributions within cavities show little if any evidence of heating or deflection although a second, suprathermal population is present. Foreshock cavities form when the enhanced pressure of suprathermal ions within bundles of field lines connected to the bow shock causes these bundles to expand outward and compress nearby plasmas and magnetic fields in regions of space not connected to the bow shock. As a result, foreshock cavities can be identified on the basis of enhanced densities and magnetic field strengths bounding regions of depressed density and magnetic field strength [*Thomas and Brecht*, 1988] containing a suprathermal ion component.

[4] The kinetic processes responsible for HFA and foreshock cavity formation are favored by long connection times with the bow shock [*Schwartz*, 1995; *Schwartz et al.*, 2000]. Consequently, near radial interplanetary magnetic field (IMF) orientations and discontinuities with normals nearly transverse to the Sun-Earth line promote the occurrence of HFAs marked by substantial amplitudes. In the absence of the multipoint measurements needed to determine event motion and orientation, it has been difficult to determine event dimensions [*Lucek et al.*, 2004].

[5] Observations concerning the kinetic aspects of foreshock cavities have not hitherto been reported. As in the case of the magnetopause [*Williams et al.*, 1979], it should be possible to use finite gyroradius effects to sense the approach and orientation of the sharp discontinuities bounding these upstream regions [*Schwartz et al.*, 1998]. In this paper, we present such observations and demonstrate that they are consistent with the motion of a narrow plane of field lines connected to the bow shock across the four Cluster spacecraft.

2. Observations

[6] We draw on data from the four Cluster spacecraft taken on 15 February 2001 when the spacecraft were located at (18.6, 5.7, 2.8)R_e GSE and separated by 500–1300 km. Magnetic field data [*Balogh et al.*, 2001] at 4s resolution were used to select the event; higher-time resolution (5 vectors/s) data were also used for multi-spacecraft time analyses. Thermal ion data from the CIS (HIA sensor) experiment [*Rème et al.*, 2001] yield both the bulk solar wind plasma parameters at spin resolution (4s) and the three-dimensional distribution functions of suprathermal ions in the range 0–32 keV every 12s. Thermal electron measurements (<26 keV) from PEACE [*Johnstone et al.*, 1997] and high energy (>35 keV) ion fluxes from RAPID [*Wilken et al.*, 2001] complete the data set used in the present work.

[7] Figure 1 summarises the magnetic field and bulk plasma parameters for an event centered at 05:30 UT. There is a clear cavity marked by depressed magnetic field strengths and densities. Field directions before and after the cavity are very similar, although the pre- and post-cavity

[1]Space and Atmospheric Physics, Blackett Laboratory, Imperial College London, London, UK.
[2]Goddard Space Flight Center, Greenbelt, Maryland, USA.
[3]Space Science Laboratory, Berkeley, California, USA.
[4]Department of Physics, University of New Brunswick, Fredericton, New Brunswick, Canada.

0094-8276/06/2005GL025612$05.00

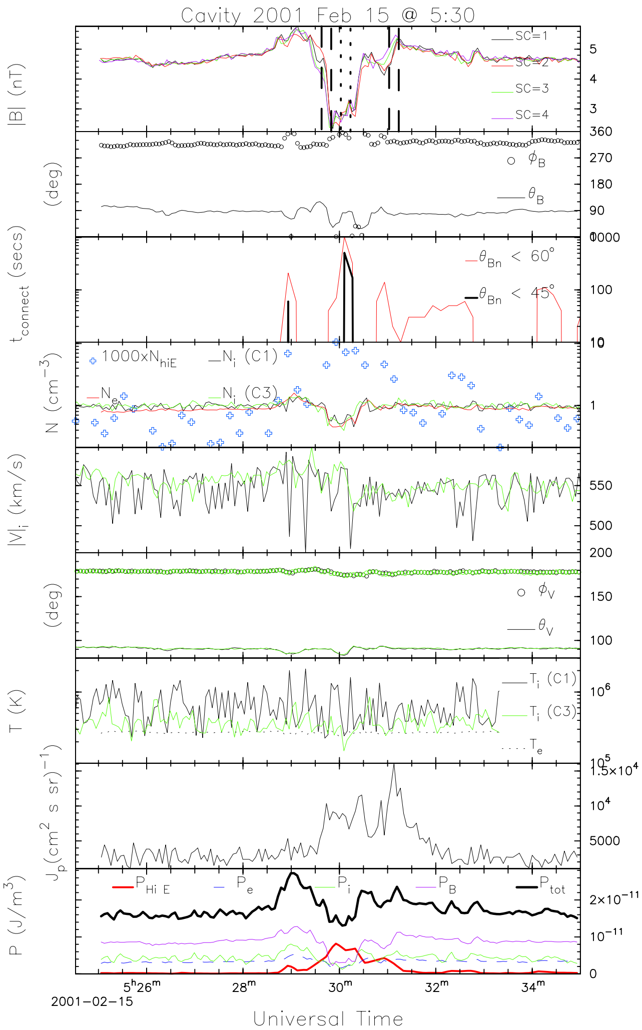

Figure 1. Overview of the plasma parameters around the foreshock cavity at 0530 on 15 February 2001 as observed by Cluster. Apart from the top panel, all parameters were measured onboard the Cluster-1 spacecraft. We also show ion moments from Cluster-3. Although neither instrument was in an optimal mode, their similar moments, and consistency with the electron density, demonstrates that the moments are adequately determined. The top two panels show the magnetic field magnitude as measured by all four spacecraft, and the orientation of the field in GSE. The third panel shows the length of time the instantaneous magnetic field line was connected to the bow shock (based on a model shape and nearby crossing) with a field-normal angle $\theta_{Bn} < 60°$ (red) and $<45°$ (black) at the intersection. Note that the center of the event was well-connected to quasi-parallel conditions for over 500 seconds. Subsequent panels show the plasma density, with symbols showing the density of the suprathermal component of ions <32 keV scaled by 1000, the bulk flow speed and direction, and temperatures of ions and electrons. The penultimate panel shows the flux of $E > 35$ keV ions measured by the RAPID instrument on Cluster. The bottom panel shows the particle and magnetic field contributions to the total plasma pressure. Note the enhanced contribution of the suprathermal ions (red) to the pressure in the core region. The locations of the distribution functions shown in Figure 2 are indicated by the dashed or dotted pairs of vertical lines in the top-most panel.

fields make an angle of 13.6°. The field at the centre of the cavity has rotated by ~30° mainly in azimuth (second panel). As a consequence, the field within the cavity is well connected to the bow shock (see third panel), which should allow for the build up of intense fluxes of suprathermal isotropic ions. Indeed, as shown in the bottom panel, the partial pressure of the suprathermal ions is greater within the event than outside and dominates the internal pressure. These suprathermal moments were computed by removing the main solar wind distribution from the 4π ion distribution.

[8] Note the enhanced densities and field strengths on the edges of the cavity. They indicate that the plasma and field lines excavated from the center pile up there, suggesting that this event is (or at least was) expanding in size. There is no significant deflection of the flow, although any such deflection might be underestimated due to the low-geometry analyser's 90° azimuthal field of view employed in the solar wind. There is also no discernable heating of either the solar wind ions or electrons (seventh panel) although a burst of energetic ions is present as shown in the penultimate panel. These ions do not contribute appreciably to the pressure. The electron velocity distributions (not shown) do not change shape appreciably although they follow the density variations through the event. Figure 1 shows that the electron temperature (seventh panel) remains constant.

[9] The suprathermal ion particle distributions exhibit clear and repeatable signatures (Figure 2). On the leading edge of the event, the ions are flowing parallel to $\vec{n} \times \vec{B}$, corresponding to ions from the cavity whose gyromotion takes them into the region adjacent to the current sheet as shown in the sketch in Figure 3. Within the weak magnetic field region and low density core of the event, a near isotropic flux is observed. At the trailing edge, the anisotropy has reversed, again as expected for the remote sensing of ions from the cavity as sketched in Figure 3. The trailing edge feature is cleaner and more persistent than the leading edge one. This would be the case if the gradient were more gradual on the trailing edge or it were traversed more slowly. There is no real evidence to support either of these suggestions. Although statistics are poorer, the same sequence of events was seen by the other spacecraft (C3) from which detailed ion distributions (not shown) were available. These remote-sensing techniques have previously been applied to more energetic particles at thin current sheets [*Meziane et al.*, 2003].

3. Interpretation

[10] We interpret the event as a foreshock cavity and not a hot flow anomaly (HFA), despite the apparently weaker HFA signatures seen in HFAs observed by Cluster [*Lucek et al.*, 2004]. Unlike HFAs, there is no significant deflection of the bulk flow in the event reported here, and the central region, while showing depressed densities and magnetic fields, is not hot. Moreover, HFAs are related to current sheets attended by substantial (typically 70°) shear in the interplanetary magnetic field [*Schwartz et al.*, 2000] which is not the case here.

[11] We have used the magnetometer observations to determine the orientation and motion of the event, and the

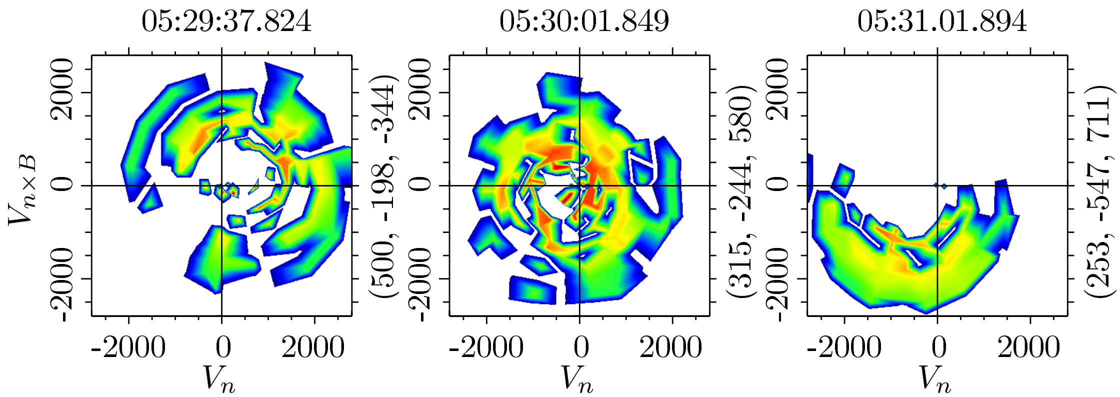

Figure 2. Cuts of the ion distributions (CIS-HIA) in a plane perpendicular to the magnetic field direction during (left) the leading portion, (center) central region, and (right) trailing portion of the foreshock cavity (all velocities in km/s) as observed onboard the Cluster 1 spacecraft. The velocity space origin is displaced by the GSE velocity vector given along the right edges. This displacement is a combination of first moving to the local bulk flow rest frame and then translating along the magnetic field direction to reach the peak fluxes in the suprathermal ion population. The horizontal axis corresponds to velocities parallel to the cavity normal, while the vertical axis are velocities along $\hat{n} \times \vec{B}$ tangential to the cavity surface. The magnetic field direction is into the page. With this definition of coordinates, remotely-sensed gyrating ions should have zero V_n and be travelling along $+\hat{n} \times \vec{B}\left(-\hat{n} \times \vec{B}\right)$ at the leading (trailing) edge, as can be seen in the left and right panels.

surfaces bounding it, via several techniques [*Schwartz*, 1998]. Since there is a finite magnetic shear from pre-event to post-event regions, assuming the underlying structure is a tangential discontinuity we can determine the normal, $\hat{n}$, simply by taking the cross product. Timings of specific, well-defined magnetic features can also be employed using the four Cluster spacecraft to determine both the normal and the speed of the feature along $\hat{n}$. As indicated in Table 1, the various vectors are consistent: they indicate a discontinuity moving antisunward, dawnward, and northward across the Cluster spacecraft. Figure 3 illustrates just such a discontinuity, with embedded magnetic fields that point sunward, dawnward, and northward.

[12] The velocity of the event ($\sim$240 km/s) across the spacecraft together with the duration of the cavity ($\sim$60s) can be used to determine its dimensions, namely $2.3 R_e$, corresponding to $\sim$3.5 gyroradii of the suprathermal particles ($v \sim 1000$ km/s) in the center of the cavity. Thus the sheet/cavity is only just thick enough to contain a region of near isotropic particles (see the middle plot of Figure 2).

[13] We have used the observed magnetic field orientations and a model bow shock to determine the length of time that each of the field lines comprising the cavity has been connected to the bow shock and the shock geometry (angle θ_{Bn}) at the point of contact. The results are shown in the third panel of Figure 1. It is clear that the field lines within the core of the event have been connected for a long period of time ($\sim$ minutes) to the quasi-parallel bow shock, while those outside the event have not. This is consistent with our understanding that a minimum amount of time is required for wave-particle interactions to build up the isotropic suprathermal particle distributions required to excavate the interior region of the cavities.

[14] At the leading and trailing edges of the discontinuity, anisotropic particle distributions are expected. As illustrated in Figure 3, the gyrovelocities of particles whose orbits extend out of the leading surface of the cavity should be in the direction $+\hat{n} \times \vec{B}$. By contrast, the gyrovelocities of particles whose orbits extend out of the trailing surface of the cavity should be in the opposite direction. These are precisely the senses observed in Figure 2 for the leading and trailing edges, as noted above. The centre of the event contains a more isotropic suprathermal ion distribution.

4. Summary

[15] We have presented detailed observations of an event upstream from the Earth's bow shock. This revealed that the prevailing solar wind conditions were those needed to produce a foreshock cavity and not a Hot Flow Anomaly based on the small change in magnetic field direction and the overall orientation of the interplanetary current sheet and

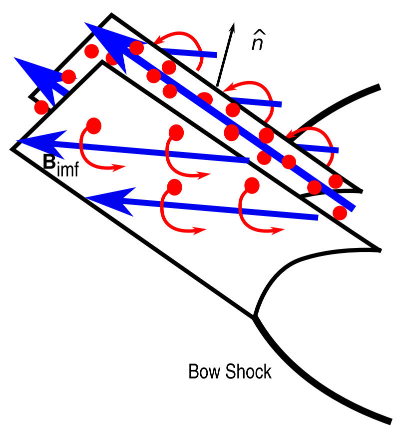

Figure 3. Sketch of the interaction of a solar wind current sheet with the bow shock forming a foreshock cavity within the current layer. Note the good, quasiparallel connection to the bow shock within the layer and the opposite gyrophases of suprathermal ions (red) on the two edges. The whole structure convects anti-sunward over the Cluster spacecraft.

Table 1. Orientation and Motion of Features

Method	Time	Normal $\hat{n}$ (GSE)	V_n, km/s
TD[a]	5:27:34, 5:32:34	(−0.545,−0.514,0.662)	-
4s/c[b]	5:28:51	(−0.604,−0.446,0.660)	248
4s/c	5:29:05	(−0.407,−0.520,0.751)	228
4s/c	5:30:37	(−0.715,−0.592,0.372)	259
Min Var[c]	5:30:37	(−0.539,−0.678,0.500)	-

[a]Tangential Discontinuity Cross Product.
[b]Four spacecraft timing analysis.
[c]Minimum Variance Cluster-1 Trailing Edge.

electric field. There was no heated, deflected flow within the event as found at well-developed HFAs.

[16] A prolonged connection to the quasi-parallel bow shock permitted the development of a flux of isotropic suprathermal ions within the core region of the event. Timing and discontinuity analyses enabled us to determine the orientation and motion of the cavity over the spacecraft. This revealed that the cavity had a thickness of $\sim 2.3 R_e$ corresponding to a few gyroradii of the suprathermal ions. However, finite gyroradius effects were expected and observed on its edges. In particular, anisotropies observed on the leading and trailing edges were in the directions expected for gyromotion about the interplanetary magnetic fields just outside the cavity.

[17] This event is not unique. We have observed similar finite gyroradius effects at the edges of an event observed some 4min later, and on other days when the spacecraft separation was much larger. Most of these events are not associated with large rotations in the interplanetary field. In each case, the orientation of the discontinuity, the particle anisotropy, and the motion of the discontinuity are consistent with expectations.

[18] **Acknowledgments.** Part of this work was supported through the generosity and hospitality of the International Space Science Institute, Berne, Switzerland. The Particle Physics and Astronomy Research Council (PPARC) provided additional support; TSH was supported by a PPARC fellowship. RAPID data were supplied courtesy Patrick Daly, PI. DS acknowledges support from NASA's Sun-Earth Connection guest investigator program.

References

Balogh, A., et al. (2001), The Cluster magnetic field investigation: Overview of in-flight performance and initial results, *Ann. Geophys.*, *19*, 1207–1217.

Johnstone, A. D., et al. (1997), PEACE: A plasma electron and current experiment, *Space Sci. Rev.*, *79*, 351–389.

Lucek, E. A., T. S. Horbury, A. Balogh, I. Dandouras, and H. Rème (2004), Cluster observations of hot flow anomalies, *J. Geophys. Res.*, *109*, A06207, doi:10.1029/2003JA010016.

Meziane, K., M. Wilber, R. P. Lin, and G. K. Parks (2003), Gyrophase-restricted 100 keV–2 MeV ion beams near the foreshock boundary, *Geophys. Res. Lett.*, *30*(20), 2049, doi:10.1029/2003GL017592.

Rème, H., et al. (2001), First multispacecraft ion measurements in and near the Earth's magnetosphere with the identical Cluster ion spectrometry (CIS) experiment, *Ann. Geophys.*, *19*, 1303–1354.

Schwartz, S. J. (1995), Hot flow anomalies near the Earth's bow shock, *Adv. Space Res.*, *15*, 107–116.

Schwartz, S. J. (1998), Shock and discontinuity normals, Mach numbers, and related parameters, in *Analysis Methods for Multi-Spacecraft Data*, edited by G. Paschmann and P. W. Daly, *ISSI Sci. Rep. SR-001*, pp. 249–270, Int. Space Sci. Inst., Bern.

Schwartz, S. J., C. P. Chaloner, D. S. Hall, P. J. Christiansen, and A. D. Johnstones (1985), An active current sheet in the solar wind, *Nature*, *318*, 269–271.

Schwartz, S. J., P. W. Daly, and A. N. Fazakerley (1998), Multi-spacecraft analysis of plasma kinetics, in *Analysis Methods for Multi-Spacecraft Data*, edited by G. Paschmann and P. W. Daly, *ISSI Sci. Rep. SR-001*, pp. 159–183, Int. Space Sci. Inst., Bern.

Schwartz, S. J., G. Paschmann, N. Sckopke, T. M. Bauer, M. Dunlop, A. N. Fazakerley, and M. F. Thomsen (2000), Conditions for the formation of hot flow anomalies at Earth's bow shock, *J. Geophys. Res.*, *105*(A6), 12,639–12,650.

Sibeck, D. G., T.-D. Phan, R. Lin, R. P. Lepping, and A. Szabo (2002), Wind observations of foreshock cavities: A case study, *J. Geophys. Res.*, *107*(A10), 1271, doi:10.1029/2001JA007539.

Sibeck, D., K. Kudela, T. Mukai, Z. Nemecek, and J. Safrankova (2004), Radial dependence of foreshock cavities: A case study, *Ann. Geophys.*, *22*, 4143–4151.

Thomas, V. A., and S. H. Brecht (1988), Evolution of diamagnetic cavities in the solar wind, *J. Geophys. Res.*, *93*, 11,341–11,353.

Thomsen, M. F., J. T. Gosling, S. A. Fuselier, S. J. Bame, and C. T. Russell (1986), Hot, diamagnetic cavities upstream from the Earth's bow shock, *J. Geophys. Res.*, *91*, 2961–2973.

Wilken, B., et al. (2001), First results from the RAPID imaging energetic particle spectrometer on board Cluster, *Ann. Geophys.*, *19*, 1355–1366.

Williams, D. J., T. A. Fritz, B. Wilken, and E. Keppler (1979), An energetic particle perspective of the magnetopause, *J. Geophys. Res.*, *84*, 6385–6396.

T. S. Horbury and S. J. Schwartz, Space and Atmospheric Physics, Blackett Laboratory, Imperial College London, South Kensington, London SW7 2BW, UK. (t.horbury@imperial.ac.uk; s.schwartz@imperial.ac.uk)

K. Meziane, Department of Physics, University of New Brunswick, Fredericton, NB, Canada E3B 5A3. (karim@unb.ca)

D. Sibeck, Goddard Space Flight Center, Greenbelt, MD 20771, USA. (dsibeck@pop600.gsfc.nasa.gov)

M. Wilber, Space Sciences Laboratory, Berkeley, CA 94620, USA. (wilber@ssl.berkeley.edu)